Letters in Applied NanoBioScience
Open-Access Journal (ISSN: 2284-6808)

Article
Volume 15, Issue 1, 2026, 33
https://doi.org/10.33263/LIANBS151.033

Multi-Targets Computational Modeling for Discovery of Potent Inhibitors from *Spondias mombin* (Linn) Stem Bark Against Breast Cancer

Damilola Alex Omoboyowa [1,*]

[1] Phyto-medicine and Computational Biology Laboratory, Department of Biochemistry, Adekunle Ajasin University, Akungba-Akoko, Ondo State, Nigeria
* Correspondence: damilola.omoboyowa@aaua.edu.ng;

Received: 5.08.2024; Accepted: 20.02.2026; Published: 30.03.2026

Abstract: Despite progress in early diagnosis and treatment strategies of breast tumour, it still remains the most prevalent type of cancer in women. Breast tumours usually exhibit intratumoral heterogeneity with estrogen receptor-positive and negative cells. Therefore, therapeutic strategies targeting the proteins that promote rapid proliferation remain a key target for drug discovery. Herein, various computational approaches were used to predict the inhibitory potential of the bioactive compounds from the n-butanol fraction of *Spondias mombin*, *previously reported by our laboratory*, against multiple proteins involved in breast cancer pathogenesis. Among these compounds, rutin, isoquercetin, rhamnetin, and quercetin were observed to be potent inhibitors of the human epidermal receptor-2 (3RCD), estrogen receptor (6CHZ), and progesterone receptor (4OAR). These compounds revealed appreciable pIC_{50} and fitness score prediction from autoQSAR and e-pharmacophore models. These compounds also showed an acceptable pharmacokinetic profile and drug-likeness properties, except for rutin and isoquercetin, which violated more than one of Lipinski's rules. Therefore, these lead compounds require *in vivo* and *in vitro* toxicity testing and experimental validation for the development of drug candidates against breast cancer.

Keywords: *in silico*; multi-target; breast cancer; flavonoids.

1. Introduction

Despite advances in rational drug design and high-throughput screening methodologies, the number of innovative, single-target medications has fallen far short of expectations [1]. Targeting a single protein related to a specific disease has several limitations, including insufficient target protein to effectively treat the disease, drug resistance, and off-target effects, which can bind and interact with other proteins unrelated to the disease [2]. Multi-target computational modeling is a computational strategy that identifies chemicals that can target numerous proteins or pathways linked with a disease using computer-based techniques [3]. Multi-target medications have stronger efficacy, a better safety profile, and are easier to administer than single-target drug combinations [4]. For the reasons stated above, "polypharmacology" or multi-targeting modeling is a growing paradigm in the therapeutic development of medications against a variety of disorders, including cancer [5].

Breast cancer remains prominent among cancers diagnosed in women globally, with an incidence that increases dramatically with age [6,7]. It is most usually diagnosed in women, with women over the age of 50 having the highest risk of developing it. Developed countries have a greater incidence rate than developing countries. Breast cancer is the leading cause of death among women worldwide [8,9]. The risk factors for breast cancer include genetic abnormalities in breast cancer-related genes such as BRCA1 and BRCA2, family history, lifestyle variables such as high-fat diets and alcohol intake, and women who have never been pregnant or had their first child at a later age [10]. Various treatment strategies for breast cancer include immunotherapy, surgery, chemotherapy, radiation therapy, and targeted therapy. However, all of these therapies have adverse effects such as fatigue, changes in the appearance of the breast, hair loss, and an increased risk of getting cancer in the treated area [11]. As a result, the creation of natural therapy with minimal side effects is required. Human epidermal receptor-2 overexpression has been attributed to the pathogenesis of breast cancer, which results in an elevated level of tumor growth and metastatic activity, thereby leading to a low survival rate and poor prognosis [12]. Breast tumors have been reported to be positive for either estrogen or progesterone receptor. Hormone receptor-positive breast cancer means the cancer cells can respond to estrogen or progesterone, which can instruct the cells to grow. The attributes of the receptors contribute to the rationale for the selection in the study.

Natural products have recently proven to be an important source of novel medications for a wide range of ailments. Popular for their low toxicity, long history of usage, and ability to target many pathways, which can lead to effective treatments with few to no side effects [13]. *Spondias mombin*, commonly known as yellow mombin or hog plum, is a tropical fruit tree native to Central and South America, well-known for its medicinal properties and traditionally used to treat a wide range of maladies [14]. In one investigation, the efficacy of *S. mombin* water extract revealed remarkable recovery for cancer-induced rats [15]. Another study found that *S. mombin* fraction rich in carotenoid potentially inhibits HER2 ATP kinase domain in HER2-positive breast cancer induced rats [16].

When compared to traditional experimental methods, the *in-silico* drug discovery strategy has proven to be an important tool in the drug development process since it can greatly shorten the time necessary and lower the resources required. This strategy identifies promising medication candidates that would be difficult or impossible to identify using traditional experimental procedures. This study is designed to apply computational tools to predict the drug-likeness of HPLC-discovered compounds from *S. mombin* against several breast cancer targets.

2. Materials and Methods

2.1. Preparation of target protein structure and ligand.

The crystallographic structures of the targets: human epidermal receptor-2 (PDB ID: 3RCD), estrogen receptor (PDB ID: 6CHZ), and progesterone receptor (PDB ID: 4OAR) were obtained from the Protein Data Bank (www.rcsb.org). The chain that contains the co-crystallized ligand was selected for the docking procedure. The target was prepared by the protein preparation wizard of the Schrodinger Maestro [17]. All of the missing residues and side chains were added during the pre-processing of the protein. The review and modification stage was used to eliminate unnecessary water molecules. The minimized protein structures were used for the docking process.

The molecule crystalized at the binding domain of each target was selected to generate the glide grid file, generating the coordinates for 3RCD: x = 13.4, y = 2.74, and z = 27.53, 6CHZ: x = -32.21, y = -2.93, and z = -23.45, and 4OAR: x = 14.22, y = 23.34, and z = 14.55.

The flavonoids identified from the n-butanol fraction of *S. mombin* via high-performance liquid chromatography (HPLC), as previously reported by Omoboyowa et al. [18], were retrieved in sdf format from the PubChem database (https://pubchem.ncbi.nlm.nih.gov), and the compounds were prepared. The Ligprep was utilized to generate energetically minimized outputs, optimize with OPLS3e force field, ionize stereoisomers, and convert to their respective 3D chemical structures at a neutral pH of 7.0 ± 2.0 using Epik [19].

2.2. Molecular docking analysis.

Molecular docking analysis of eight compounds obtained from the HPLC analysis of the n-butanol fraction of *S. mombin* was carried out using the GLIDE docking module on Schrodinger. Prior to docking, the docking procedure was validated for reproducibility and accuracy for all the targets. The molecule co-crystalized with the proteins was removed from the binding domain, prepared, and re-docked into the same catalytic site of 3RCD, 6CHZ, and 4OAR.

Molecular docking was carried out using GLIDE-extra precision (XP) procedure. XP was adopted because it is a discriminating and robust protocol that can run for longer than other precision techniques. It is also used to eliminate false-positive results [20]. Following that, the ligands were classified according to their binding affinities. The Ligand-protein interactions were exported to Discovery Studio 2020 to build the 2D interaction profile of protein-ligand complexes.

2.3. MM-GBSA and binding free energy.

The binding free energies of the XP-screened compounds and the reference drug were determined using the MM-GBSA module of the Schrodinger software. The docked ligand-target complexes were minimized with the local optimization feature in Prime. The binding energy (ΔG^{bind}) for the complexes was predicted by employing the OPLS3 force field [21]. The equation below was used to estimate the binding free energy:

$$\Delta G^{bind} = \Delta E^{MM} + \Delta G^{solv} + \Delta G^{SA} \qquad (1)$$

2.4. Generation of E-pharmacophore hypothesis and phase screening of compounds.

The E-pharmacophore hypothesis was generated for the targets (3RCD, 6CHZ, and 4OAR) with co-crystalized ligands through the energy-optimized receptor-ligand pharmacophore of Maestro Suite (2007-1). The compounds were prepared with macromodel minimization and screened by E-pharmacophore-based phase screening of the generated subset of compounds that possess the requisite features for the target binding to the targets. Overall, the fitness scores of the compounds were estimated [22].

2.5. AutoQSAR model generation.

Experimental data for the inhibitors of the targets (3RCD, 6CHZ, and 4OAR) were retrieved from www.ebi.ac. uk/chembl/ (CHEMBL database) along with their pIC50 values. Data-warrior (v-2) was used to convert the dataset to their sdf format [23]. These files were imported into the Schrodinger workspace, followed by preparation with the Macromodel tool. The autoQSAR models of the proteins were generated according to the hit compounds' pIC_{50}. The best-ranked models based on the outcome were selected to screen the pIC_{50} of the compounds.

2.6. Prediction of the pharmacokinetic and drug-likeness properties.

The pharmacokinetics (QPlogHERG, QPPCaco, QPlogKhsa, % Oral Absorption) and drug-likeness profile of the compounds were screened by the Qikprop tool of Schrodinger Suite (v11.12) [24].

3. Results and Discussion

3.1. Analysis of the docking score and binding free energy.

To validate the docking protocol in this study, co-crystalized ligands from the protein were removed, prepared, and re-docked into the catalytic site of the targets. The deviation of the re-docked ligands and the co-crystalized ligands was estimated as root mean square deviations (RMSD), which were observed to be 1.692 Å, 1.432 Å, and 0.647 Å for 3RCD, 6CH, and 4OAR, respectively. The RMSD of the targets was less than 2 Å, which suggests the reliability of the docking protocol [20,12]. The co-crystalized ligands (green) superimposed with the re-docked ligands (red) at the binding site of the targets (3RCD, 6CH, and 4OAR) are shown in Figure 1.

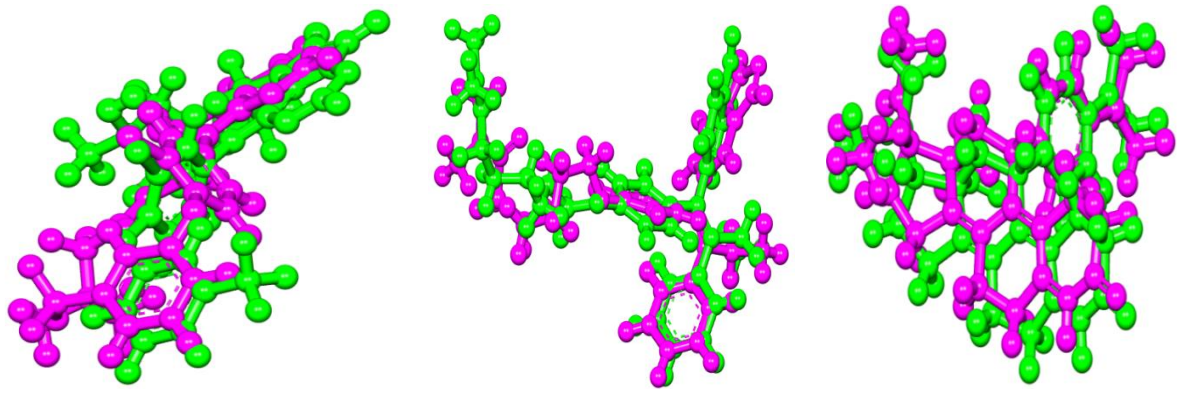

(a) **(b)** **(c)**

Figure 1. Docked pose of superimposition of targets and co-crystalized ligand **(a)** 3RCD; **(b)** 6CHZ; **(c)** 4OAR.

Molecular docking is an important protocol for studying the mechanisms of interaction and binding of small molecules to the catalytic site of targets during drug design [25]. Inhibitory potential of bioactive compounds identified from butanol fraction of *S. mombin* stem bark previously reported in our lab [18] against human epidermal receptor-2 (3RCD), estrogen receptor (6CH), and progesterone receptor (4OAR) involved in human breast cancer was predicted according to the binding analysis using extra precision filtering screening and energy calculation.

The binding score and free energy predictions are represented in Figure 2. The higher the binding score, the better the binding affinity. Hence, rutin, isoquercetin, rhamnetin, and quercetin identified from the fraction were observed to favourably bind to the three targets (3RCD, 6CH, and 4OAR) compared to the reference drug (Gefitinib). Therefore, these four compounds are classified as lead compounds. The binding score of the lead compounds ranges from -9.450 kcal/mol to -14.568 kcal/mol.

Four (4) lead compounds from *S. mombin* stem bark were observed to potentially inhibit breast cancer, considering the binding scores. Previous studies have reported the inhibitory potential of small molecules against estrogen receptor [26,27]. The human epidermal receptor-2 (HER-2) inhibitory activity of *S. mombin* molecules reported in this study is consistent with a previous study by Balogun et al. [12], who reported potential HER-2 inhibitors from *Mangifera indica.* The inhibitory activity of the flavonoids from *S. mombin* stem bark reported in this study also agrees with the findings of Suganya et al. [27], who reported the inhibitory potential of selected flavonoids against estrogen receptors. Zarezade et al. [28] have also reported the inhibitory potential of natural compounds against progesterone receptors as a new insight into the treatment of breast cancer.

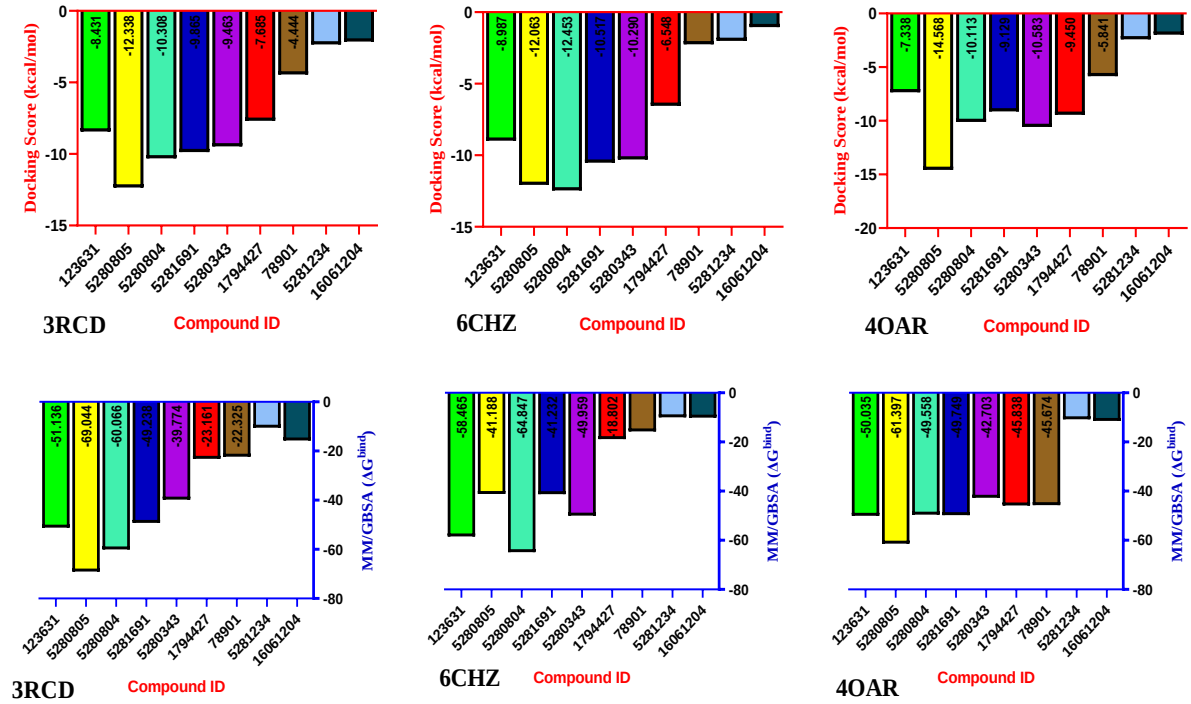

Figure 2. Representation of the docking affinity and binding free energy (ΔG^{bind}) of hits. 123631-Gefitinib; 5280805 - Rutin; 5280804 - Isoquercetin; 5281691- Rhamnetin; 5280343- Quercetin; 1794427 – Chlorogenic acid; 78901 - Rutinose; 5281234 - Zeinoxanthin; 16061204 – Lutein.

The interaction of natural compounds with amino acids surrounding the catalytic domain of the target is important for predicting the potential of these molecules to inhibit the protein. The active sites of the targets consist of some essential residues that contribute to the binding of Ligand-protein complexes. As revealed in Figure 3, the hit compounds were thoroughly studied for their binding with the amino acids. The 2-dimensional representation of the interactions revealed that isoquercetin and rutin formed five (5) and eight (8) H-bond interactions with HER-2 involving ASP 808, ARG 849, MET 801, GLN 799, CYS 805, ASN

850, and LYS 753. Isoquercetin and rutin also showed five (5) and four (4) H-bond interactions, respectively, with estrogen receptor involving GLY 521, ASP 351, THR 347, LEU 346, GLU 352, MET 343 at the binding site of the protein. Progesterone receptor forms five (5) and three (3) H-bonds with isoquercetin and rutin, respectively, using LEU 887, MET 756, GLN 725, and LEU 718. The formation of hydrogen bonds between the hit compounds and the targets' binding domains could result from the functional groups on the flavonoids, which might contribute to the binding affinity of the complexes [29].

Molecular mechanics generalized born surface area is a common model for estimating the free energy binding of ligand-protein complexes [30]. MM/GBSA is known for its accurate prediction among other scoring functions of molecular docking [31]. The docking results revealed that the compounds interact with amino acid residues at the active site of the targets. However, the ability of the interactions to elicit sufficient biological response can be determined by the free binding energies of the protein-ligand complexes. Hence, the validation of the docking analysis was corroborated by the MM/GBSA evaluation. The free energy result predicted in this work is represented in Figure 3. Among the lead compounds, the Rutin-3RCD and Isoquercetin-3RCD complexes showed the highest binding free energy, exceeding that of the Gefitinib-3RCD complex. Hence, the docking affinities were comparable with the binding free energy of the lead compound-target complexes.

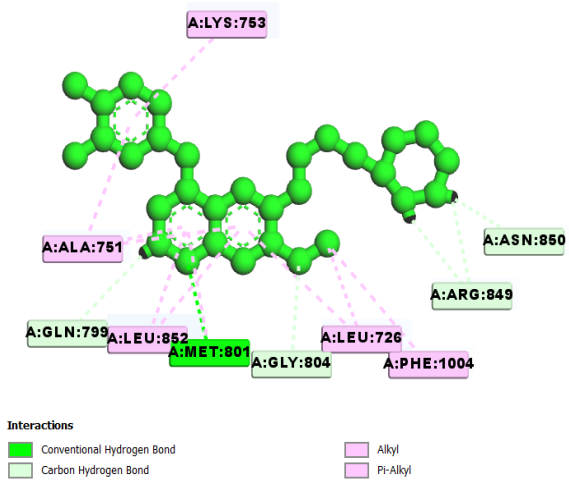

3RCD-123631

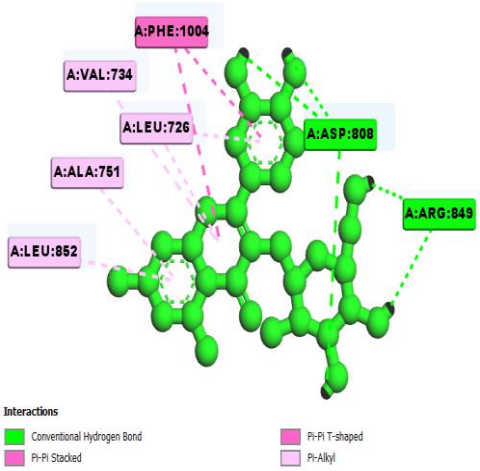

3RCD-5280804

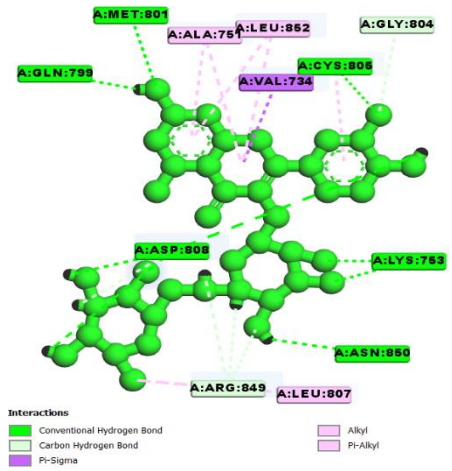

3RCD-5280805

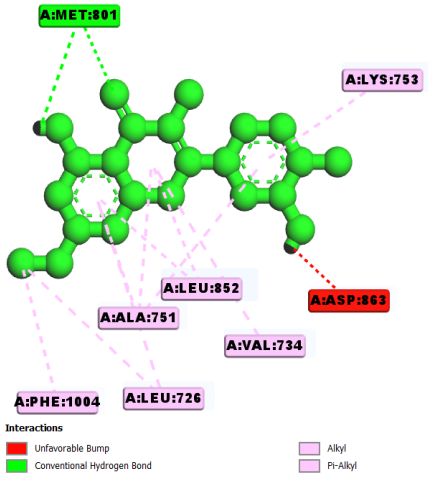

3RCD-5281691

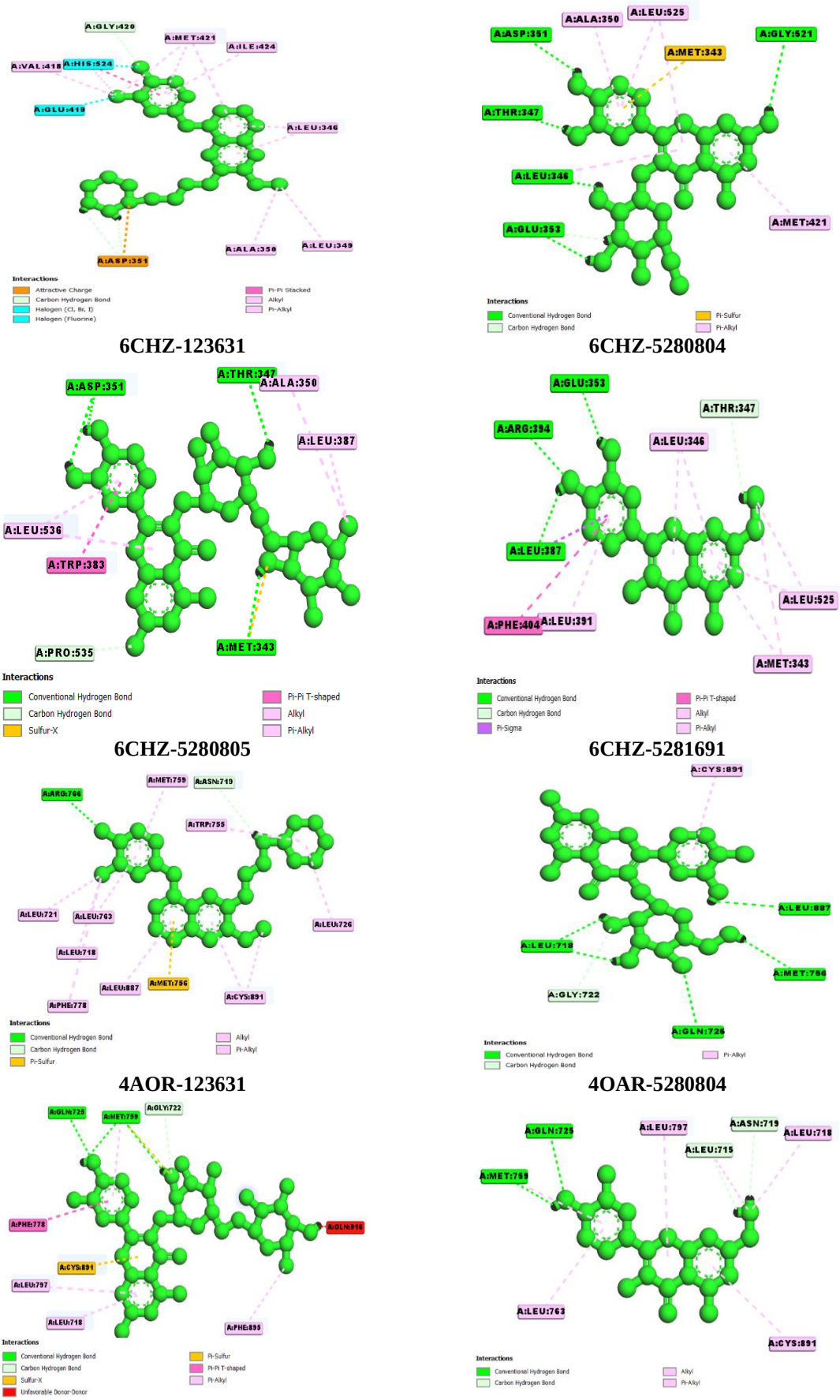

Figure 3. 2D molecular interaction of bioactive compounds with binding pocket amino acids of the targets, viz. 3RCD: Human epidermal receptor-2; 6CHZ: Estrogen receptor; 4OAR: Progesterone receptor; Gefitinib; 5280805 - Rutin; 5280804 - Isoquercetin; 5281691- Rhamnetin; 5280343- Quercetin; 1794427 – Chlorogenic acid; 78901 - Rutinose; 5281234 - Zeinoxanthin; 16061204 – Lutein.

3.2. E-pharmacophore model generation.

The hypothesis of a ligand-based pharmacophore is an electronic ensemble and steric features that are vital in computational drug discovery without the protein structure, interacting with specific biological macromolecules to inhibit signaling pathways [32,33]. In this study, e-pharmacophore models of the targets (3RCD, 6CHZ, and 4OAR) were generated using the co-crystalized ligand. Hypothesis identification was carried out using four partitioning features. Figure 4 represents the hypotheses generated from the target-co-crystalized complex. The best hypothesis was selected based on features such as one aromatic ring, one hydrogen bond acceptor, a hydrophobic interaction, and two hydrogen bond donors. The identified compounds from *S. mombin* bark were screened based on these features.

The fitness score of the eight (8) compounds and the reference drug is shown in Table 1. The reference drug (Gefitinib) against the human epidermal receptor-2 (3RCD) showed a higher fitness score (1.742) than all the bioactive compounds. Isoquercetin was observed to have the highest fitness score among the bioactive compounds across the three targets (3RCD = 1.574, 6CHZ = 1.541, and 4OAR = 1.760). The fitness scores of isoquerdcetin against 6CHZ and 4OAR were shown to be higher than the reference drug (Gefitinib). Therefore, Isoquercetin might be regarded as the best among the bioactive compounds based on the pharmacophore hypothesis.

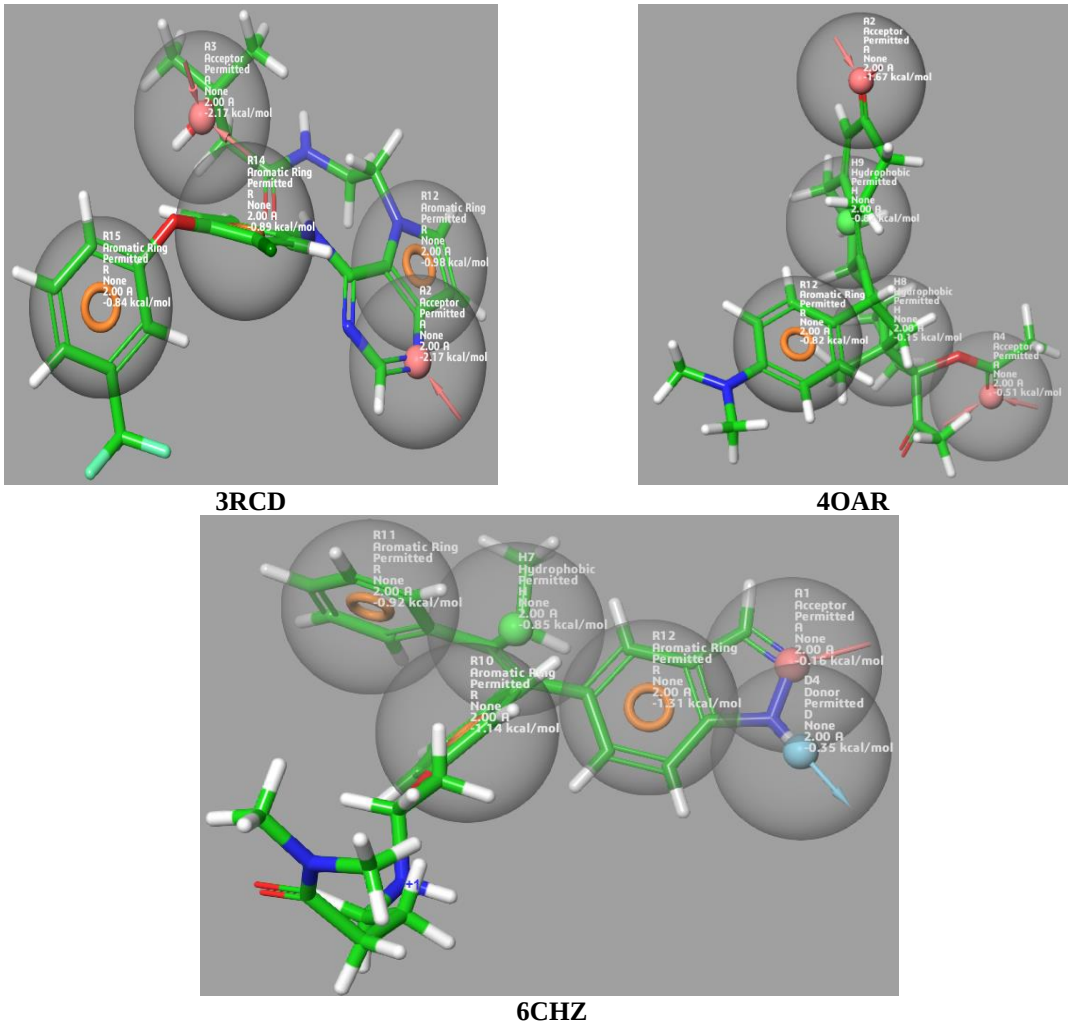

Figure 4. Hypothesis generated from the target-co-crystalized molecule complex.

Table 1. Predicted fitness scores of hit compounds.

Pubchem ID	Compound Name	Fitness Score		
		3RCD	6CHZ	4OAR
123631	Gefitinib (Ref. drug)	1.742	1.198	1.650
5280805	Rutin	1.166	0.935	0.849
5280804	Isoquercetin	1.574	1.541	1.760
5281691	Rhamnetin	1.476	1.484	1.195
5280343	Quercetin	1.463	1.492	0.000
1794427	Chlorogenic Acid	1.408	1.288	0.000
78901	Rutinose	0.000	0.000	0.000
5281234	Zeinoxanthin	0.000	0.000	1.495
16061204	Lutein	0.000	1.095	1.525

3.3. Auto QSAR analysis.

Quantitative structure-activity relationship is an important computational model in drug discovery that defines the relationship between the structural characteristics of low-molecular-weight molecules and their biological activities [34,35], based on predictive models derived from the QSAR hypothesis and experimental data generated on the targets. The best model from each target was selected with the predicted activity against the observed activity scatter graph shown in Figure 5, as the models showing less of the test set (red) compared with the train set (blue). The predictive model indices predicted for the targets are shown in Table 2. The QSAR models were used to obtain the pIC_{50} of the bioactive compounds shown in Table 3. The pIC_{50} range of the compounds against 3RCD, 6CHZ, and 4OAR is 4.801-6.868 µM, 8.685 – 9.139 µM, and 4.826 – 5.760 µM, respectively. All the bioactive compounds showed higher pIC50 values against 6CHZ compared with other targets.

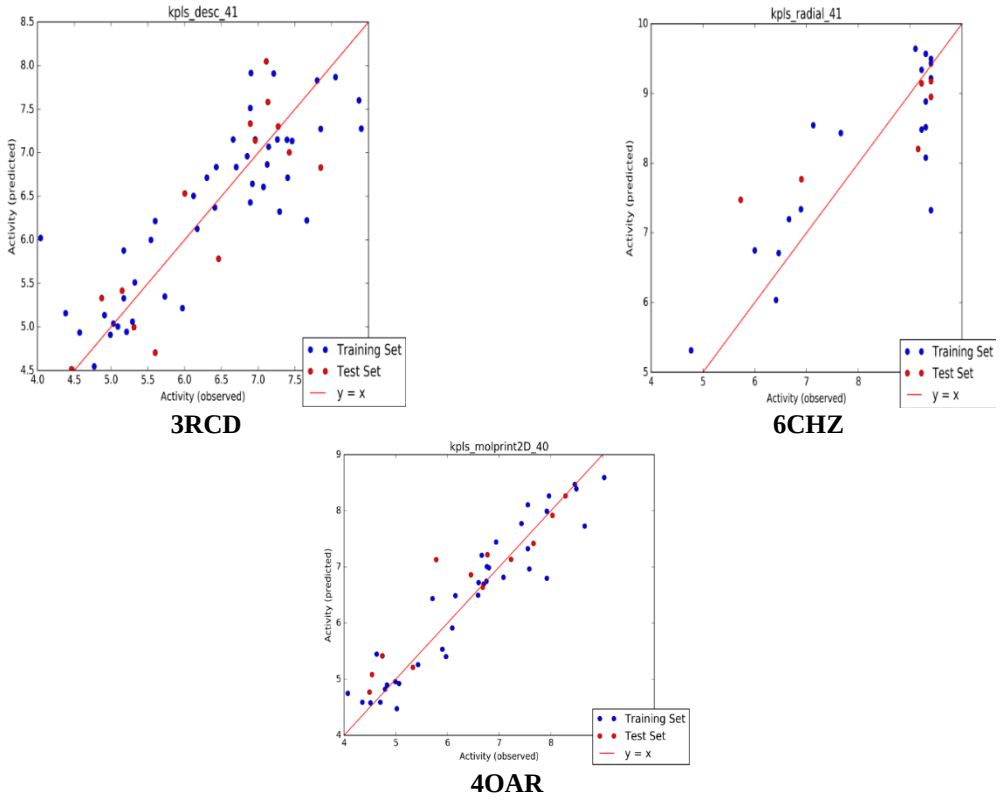

Figure 5. Graphical representation of the best model.

Gefitinib (reference drug) showed higher pIC50 against 3RCD and 6CHZ (6.868 and 9.139 µM, respectively) than the bioactive compounds. Among the compounds, thamnetin

showed the highest pIC_{50} against 3RCD (5.437 µM) and 6CHZ (8.977 µM), and zeinoxanthin was observed to have the highest pIC_{50} (5.760 µM) against 4OAR.

Table 2. AutoQSAR indices of the corresponding best hypothesis.

Protein ID	Model code	S.D	R^2	RMSE	Q^2
3RCD	kpls_desc_41	0.6228	0.7216	0.5639	0.7044
6CHZ	Kpls_radial_41	0.8297	0.7196	0.9087	0.6053
4OAR	Kpls_molprint2D_40	0.4504	0.8987	0.5105	0.8438

Table 3. pIC_{50} predicted for the compounds according to the best model.

Pubchem ID	Compound Name	Predicted IC_{50} (µM)		
		3RCD	6CHZ	4OAR
123631	Gefitinib (Ref. drug)	6.868	9.139	4.901
5280805	Rutin	5.148	8.833	5.029
5280804	Isoquercetin	5.422	8.740	5.014
5281691	Rhamnetin	5.437	8.977	4.826
5280343	Quercetin	5.347	8.669	4.967
1794427	Chlorogenic Acid	4.921	8.941	5.088
78901	Rutinose	5.207	8.685	5.631
5281234	Zeinoxanthin	4.801	8.860	5.760
16061204	Lutein	4.828	8.759	5.689

3.4. Compounds' pharmacokinetic profile and drug-likeness study.

Natural compounds with therapeutic potential fail at clinical trials due to undesirable pharmacokinetic evaluation [36]. Therefore, determining the pharmacokinetic profile of small molecules is vital in drug design, and computational pharmacokinetic modeling provides a cost-effective and rapid approach for evaluating the safety of large compounds. Drug likeness remains the primary qualitative method for predicting the likelihood that a molecule will become a drug candidate. Lipinski's rule of five (ROV) is a popular rule for determining druggability drug ability of small molecules using the following criteria: acceptor hydrogen bond of less than 10 (HBA < 10), molecular weight of less than 500 Da (MW < 500 Da), donor hydrogen bond of less than 5 (HBD < 5), and octanol-water partition coefficient less than 5 (LogP < 5) [37]. The results from this study showed that quercetin and rhamnetin obey all the Lipinski rules of five, whereas lutein, chlorogenic acid, and zeinoxanthin violated one of the ROV (Table 4), suggesting that all five (5) compounds are therapeutic agents. While rutinose, isoquercetin, and rutin violated more than one rule of five, suggesting low oral bioavailability for these compounds.

The pharmacokinetic status of the compounds was determined using apparent calcium carbonate (QPCaco), brain/blood partition coefficient ($QPlog^{BB}$), blockage of HERG K ($QPLog^{HERG}$), and human serum albumin binding ($QPlog^{khsa}$), as presented in Table 5. Human serum albumin remains a prominent protein in plasma known for its exceptional binding ability to ligands [38]. All the compounds were observed to be binding with serum albumin with the value of $QPlog^{khsa}$ within the normal range. The rapid membrane permeability screening of the compounds was predicted using the MDCK cell model [39]. Rutin and isoquercetin had the lowest predicted scores, -4.728 and -3.388, respectively, for blood-brain barrier (BBB) penetration. The blood-brain barrier partition coefficient remains a potential predictor of the ability of drugs to cross the nervous system. The hERG K^+ channel is used for normal electrical activity [40]. The $QPLog^{HERG}$ is toxic; therefore, the IC_{50} value for QP^{HERG} is one of the vital steps of drug discovery. Zeinoxanthin and lutein showed $QPLog^{HERG}$ value less than -5.5, while other compounds have QPlogHERG values within the normal range (above -5.5). Hence,

zeinoxanthin and lutein could be slightly cardiotoxic. However, the slight cardiotoxic potential of these compounds(zeinoxanthin and lutein), as indicated by their QPlogHERG values, suggests that the plant should be used at low concentration for short duration to avoid unwanted side effects.

Table 4. Prediction of drug-likeness of bioactive compounds.

Compounds	MW	HBA	HBD	ALogP	PSA	ROV
Lutein	568.87	2	2	3.43	40.46	1
Rutinose	620.55	17	0	4.26	211.79	2
Chlorogenic Acid	354.31	9	6	0.87	164.75	1
Quercetin	302.24	7	5	2.531	131.36	0
Isoquercetin	464.38	12	8	0.94	210.51	2
Rutin	610.52	16	10	0.46	269.43	3
Zeinoxanthin	552.87	1	1	4.23	20.23	1
Rhamnetin	316.26	7	4	2.23	120.36	0

Molecular weight (MW); Hydrogen Bond acceptor (HBA); Hydrogen Bond donor (HBD), Polar Surface Area (PSA); Rules of five (ROV).

Table 5. Pharmacokinetic status of compounds.

Compound Name	QPlogHERG	QPPCaco	QPlogBB	QPlogKhsa	HOA (%)
Lutein	-7.214	1127.146	-2.020	2.871	100
Rutinose	-5.209	217.792	-1.991	-1.781	44.769
Chlorogenic Acid	-3.279	1.701	-3.323	-0.91	16.816
Quercetin	-5.109	18.199	-2.419	-0.343	51.655
Isoquercetin	-4.854	4.013	-3.388	-0.848	4.147
Rutin	-5.288	0.691	-4.728	-1.273	0
Zeinoxanthin	-7.177	3377.931	-1.260	3.357	100
Rhamnetin	-5.152	60.046	-1.945	-0.157	65.916

HOA: Human oral absorption.

4. Conclusions

Human epidermal receptor (3RCD), estrogen receptor (6CHZ), and progesterone receptor (4OAR) are therapeutic targets for breast cancer. Hence, this study has predicted the inhibitory potential of bioactive compounds identified from Spondias mombin as a promising antagonist of multiple proteins involved in breast cancer pathogenesis via a computational approach. Four (4) lead compounds (Rutin, Isoquercetin, Rhamnetin, and Quercetin) were observed to show antagonistic potential with acceptable pharmacokinetic profiles, although rutin and isoquercetin violated more than one Lipinski rule of five. Importantly, to the best of our knowledge, the application of these bioactive constituents from *Spondias mombin*, particularly Rhamnetin and Isoquercetin, targeting breast cancer-related receptors has not been extensively explored. This highlights the novelty of the findings and supports the relevance of further experimental validation. Therefore, the isolation of these compounds and their evaluation *in vitro* using breast cancer cell lines, as well as *in vivo* using suitable animal models, are recommended to substantiate their potential as novel anti-breast cancer agents.

Author Contributions

Conceptualization, D. A. O.; Methodology, D. A. O.; Software, D. A. O.; Validation, D. A. O.; Investigation, D. A. O.; Data curation, D. A. O.; Writing – original draft, D. A. O.; Visualization, D. A. O. The author has read and agreed to the published version of the manuscript.

Institutional Review Board Statement

Not applicable.

Informed Consent Statement

Not applicable.

Data Availability Statement

Data supporting the findings of this study are available upon reasonable request from the corresponding author.

Funding

This research received no external funding.

Acknowledgments

The author would like to thank the Department of Biochemistry, Adejunle Ajasin University, Akungba-Akoko, for providing the Schrodinger software used for the computational modeling.

Conflicts of Interest

The authors declare no conflict of interest.

References

1. Korcsmáros, T.; Szalay, M.S.; Böde, C.; Kovács, I.A.; Csermely, P. How to design multi-target drugs. *Expert Opin. Drug Discov.* **2007**, *2*, 799-808, https://doi.org/10.1517/17460441.2.6.799.
2. Csermely, P.; Ágoston, V.; Pongor, S. The efficiency of multi-target drugs: the network approach might help drug design. *Trends Pharmacol. Sci.* **2005**, *26*, 178-182, https://doi.org/10.1016/j.tips.2005.02.007.
3. Oleg, A.R.; Azat, M.; Veniamin, Y.G.; Alexey, U.; Shwu-Chen, T.; Reuben Jih-Ru, H.; Nagendra Sastry, Y.; Vadim, V.T.; Gjumrakch, A.; Sergey, O.B. Applications of Multi-Target Computer-Aided Methodologies in Molecular Design of CNS Drugs. *Curr. Med. Chem.* **2018**, *25*, 5293-5314, https://doi.org/10.2174/0929867324666170920154111.
4. Zhang, W.; Pei, J.; Lai, L. Computational Multitarget Drug Design. *J. Chem. Inf. Model.* **2017**, *57*, 403-412, https://doi.org/10.1021/acs.jcim.6b00491.
5. Stelitano, G.; Sammartino, J.C.; Chiarelli, L.R. Multitargeting Compounds: A Promising Strategy to Overcome Multi-Drug Resistant Tuberculosis. *Molecules* **2020**, *25*, 1239, https://doi.org/10.3390/molecules25051239.
6. Abdullahi, S.H.; Uzairu, A.; Shallangwa, G.A.; Uba, S.; Umar, A.B. In-silico activity prediction, structure-based drug design, molecular docking and pharmacokinetic studies of selected quinazoline derivatives for their antiproliferative activity against triple negative breast cancer (MDA-MB231) cell line. *Bull. Natl. Res. Cent.* **2022**, *46*, 2, https://doi.org/10.1186/s42269-021-00690-z.
7. Giordano, S.H.; Buzdar, A.U.; Hortobagyi, G.N. Breast Cancer in Men. *Ann. Intern. Med.* **2002**, *137*, 678-687, https://doi.org/10.7326/0003-4819-137-8-200210150-00013.
8. Padegimas, A.; Clasen, S.; Ky, B. Cardioprotective strategies to prevent breast cancer therapy-induced cardiotoxicity. *Trends Cardiovasc. Med.* **2020**, *30*, 22-28, https://doi.org/10.1016/j.tcm.2019.01.006.
9. Dibden, A.; Offman, J.; Duffy, S.W.; Gabe, R. Worldwide Review and Meta-Analysis of Cohort Studies Measuring the Effect of Mammography Screening Programmes on Incidence-Based Breast Cancer Mortality. *Cancers* **2020**, *12*, 976, https://doi.org/10.3390/cancers12040976.
10. Momenimovahed, Z.; Salehiniya, H. Epidemiological characteristics of and risk factors for breast cancer in the world. *Breast Cancer: Targets Ther.* **2019**, *11*, 151-164, https://doi.org/10.2147/BCTT.S176070.

11. Chang, L.; Weiner, L.S.; Hartman, S.J.; Horvath, S.; Jeste, D.; Mischel, P.S.; Kado, D.M. Breast cancer treatment and its effects on aging. *J. Geriatr. Oncol.* **2019**, *10*, 346-355, https://doi.org/10.1016/j.jgo.2018.07.010.
12. Balogun, T.A.; Iqbal, M.N.; Saibu, O.A.; Akintubosun, M.O.; Lateef, O.M.; Nneka, U.C.; Abdullateef, O.T.; Omoboyowa, D.A. Discovery of potential HER2 inhibitors from *Mangifera indica* for the treatment of HER2-Positive breast cancer: an integrated computational approach. *J. Biomol. Struct. Dyn.* **2022**, *40*, 12772-12784, https://doi.org/10.1080/07391102.2021.1975570.
13. Antonio, A.d.S.; Wiedemann, L.S.M.; Veiga-Junior, V.F. Natural products' role against COVID-19. *RSC Adv.* **2020**, *10*, 23379-23393, https://doi.org/10.1039/D0RA03774E.
14. Ogunro, O.B.; Oyeyinka, B.O.; Gyebi, G.A.; Batiha, G.E.-S. Nutritional benefits, ethnomedicinal uses, phytochemistry, pharmacological properties and toxicity of *Spondias mombin* Linn: a comprehensive review. *J. Pharm. Pharmacol.* **2023**, *75*, 162-226, https://doi.org/10.1093/jpp/rgac086.
15. Ataman, J.E.; Idu, M.; Okoro, M.A.; Akinbo, S.F.; Ayinde, B.A.; Ibe, N.I.; Idu, F.K.; Akhigbe, A.O.; Omoregie, E.S. Preliminary studies on the phytochemistry and efficacy of extracts of the bark of *Spondias mombin* l. on induced cancer in rats. *Ann. Biomed. Sci.* **2008**, *1*, 100-110, https://doi.org/10.4314/abs.v1i2.40629.
16. Metibemu, D.S.; Akinloye, O.A.; Omotuyi, I.O.; Okoye, J.O.; Popoola, M.A.; Akamo, A.J. Carotenoid-Enriched Fractions From Spondias mombin Demonstrate HER2 ATP Kinase Domain Inhibition: Computational and In Vivo Animal Model of Breast Carcinoma Studies. *Front. Oncol.* **2021**, *11*, 687190, https://doi.org/10.3389/fonc.2021.687190.
17. Release 2018-4, Maestro Schrödinger, LLC, New York, NY, **2018**.
18. Omoboyowa, D.A.; Agoi, M.D.; Shodehinde, S.A.; Saibu, O.A.; Saliu, J.A. Antidiabetes study of *Spondias mombin* (Linn) stem bark fractions in high-sucrose diet-induced diabetes in *Drosophila melanogaster*. *J. Taibah Univ. Med. Sci.* **2023**, *18*, 663-675, https://doi.org/10.1016/j.jtumed.2023.01.011.
19. Bodun, D.S.; Omoboyowa, D.A.; Adedara, J.F.; Olugbogi, E.A.; Oluwamoroti, F.O.; Atasie, N.H.; Oluwafemi, I.O. Virtual screening of flavonoids from Blighia sapida against ERK5 involved in breast cancer. *Proc.Indian Natl. Sci. Acad.* **2023**, *89*, 957-966, https://doi.org/10.1007/s43538-023-00210-9.
20. Omoboyowa, D.A. Exploring molecular docking with E-pharmacophore and QSAR models to predict potent inhibitors of 14-α-demethylase protease from *Moringa spp*. *Pharmacol. Res. - Mod. Chin. Med.* **2022**, *4*, 100147, https://doi.org/10.1016/j.prmcm.2022.100147.
21. Al-Fahad, D.; Ropón-Palacios, G.; Omoboyowa, D.A.; Singh, G.; Patil, R.B. Virtual screening and molecular dynamics simulation of natural compounds as potential inhibitors of serine/threonine kinase 16 for anticancer drug discovery. *Mol. Divers.* **2025**, *29*, 1525-1539, https://doi.org/10.1007/s11030-024-10931-8.
22. Omoboyowa, D.A.; Iqbal, M.N.; Balogun, T.A.; Bodun, D.S.; Fatoki, J.O.; Oyeneyin, O.E. Inhibitory potential of phytochemicals from *Chromolaena odorata* L. against apoptosis signal-regulatory kinase 1: A computational model against colorectal cancer. *Comput. Toxicol.* **2022**, *23*, 100235, https://doi.org/10.1016/j.comtox.2022.100235.
23. Sofela, S.O.; Bodun, D.S.; Omoboyowa, D.A.; Ajiboro, P.A.; Nwankwo, D.O.; Ashimiyu-Abdusalam, Z.; Issac, I.B.; Abdulrasheed, B.; Balogun, T.A.; Ajayi, I.H. Virtual screening for novel FGFR2 inhibitors: Exploring Gefitinib-like compounds as promising therapeutic candidates. *Inform. Med. Unlocked* **2023**, *42*, 101368, https://doi.org/10.1016/j.imu.2023.101368.
24. Omoboyowa, D.A.; Kareem, J.A.; Saibu, O.A.; Bodun, D.S.; Ajayi, T.M.; Oyeneyin, O.E. Identification of Phyto-Compounds from *Ilex kudingcha* as Inhibitors of Sterol-14α-Demethylase Protease: A Computational Approach Against Chagas Disease. *Chem. Africa* **2023**, *6*, 1335-1347, https://doi.org/10.1007/s42250-022-00565-4.
25. Aribigbola, T.C.; Omoboyowa, D.A.; Bodun, D.S. Computational prediction of 11β-hydroxysteroid dehydrogenase inhibitors from n-butanol fraction of *Blighia welwetschii* (Hiern) leaf for the management of type-2 diabetes. *J. Biomol. Struct. Dyn.* **2024**, *42*, 10272-10285, https://doi.org/10.1080/07391102.2023.2256869.
26. Begam, J.A.; Basheer, A.; Jubie, S.; Dhanabal, S.P. An in-silico study of novel coumarin analogues as huamn estrogen receptor inhibitors. *J. Pharm. Sci. Res.* **2017**, *9*, 1953-1957.
27. Suganya, J.; Radha, M.; Naorem, D.L.; Nishandhini, M. *In Silico* Docking Studies of Selected Flavonoids - Natural Healing Agents against Breast Cancer. *Asian Pac. J. Cancer Prev.* **2014**, *15*, 8155-8159.

28. Zarezade, V.; Abolghasemi, M.; Rahim, F.; Veisi, A.; Behbahani, M. In silico assessment of new progesterone receptor inhibitors using molecular dynamics: a new insight into breast cancer treatment. *J. Mol. Model.* **2018**, *24*, 337, https://doi.org/10.1007/s00894-018-3858-6.
29. Omoboyowa, D.A.; Bodun, D.S.; Saliu, J.A. Structure-based *in silico* investigation of antagonists of human ribonucleotide reductase from *Annona muricata*. *Inform. Med. Unlocked* **2023**, *38*, 101225, https://doi.org/10.1016/j.imu.2023.101225.
30. Godschalk, F.; Genheden, S.; Söderhjelm, P.; Ryde, U. Comparison of MM/GBSA calculations based on explicit and implicit solvent simulations. *Phys. Chem. Chem. Phys.* **2013**, *15*, 7731-7739, https://doi.org/10.1039/C3CP00116D.
31. Wang, E.; Sun, H.; Wang, J.; Wang, Z.; Liu, H.; Zhang, J.Z.H.; Hou, T. End-Point Binding Free Energy Calculation with MM/PBSA and MM/GBSA: Strategies and Applications in Drug Design. *Chem. Rev.* **2019**, *119*, 9478-9508, https://doi.org/10.1021/acs.chemrev.9b00055.
32. Yang, S.-Y. Pharmacophore modeling and applications in drug discovery: challenges and recent advances. *Drug Discov. Today* **2010**, *15*, 444-450, https://doi.org/10.1016/j.drudis.2010.03.013.
33. Muhammed, M.T.; Akı-yalcın, E. Pharmacophore Modeling in Drug Discovery: Methodology and Current Status. *J. Turk. Chem. Soc. Sect. A Chem.* **2021**, *8*, 749-762, https://doi.org/10.18596/jotcsa.927426.
34. Kwon, S.; Bae, H.; Jo, J.; Yoon, S. Comprehensive ensemble in QSAR prediction for drug discovery. *BMC Bioinform.* **2019**, *20*, 521, https://doi.org/10.1186/s12859-019-3135-4.
35. Albratty, M. Quantitative structure–activity relationship modeling and docking of some synthesized bioactive oxopyrolidines against *Staphylococcus aureus*. *J. Saudi Chem. Soc.* **2022**, *26*, 101509, https://doi.org/10.1016/j.jscs.2022.101509.
36. Omoboyowa, D.A.; Omomule, O.M.; Balogun, T.A.; Saibu, O.A.; Metibemu, D.S. Protective potential of ethylacetate extract of *Abrus precatorius (*Linn) seeds against HCl/EtOH-induced gastric ulcer via pro-inflammatory regulation: *In vivo* and *in silico* study. *Phytomed. Plus* **2021**, *1*, 100145, https://doi.org/10.1016/j.phyplu.2021.100145.
37. Lipinski, C.A.; Lombardo, F.; Dominy, B.W.; Feeney, P.J. Experimental and computational approaches to estimate solubility and permeability in drug discovery and development settings. *Adv. Drug Deliv. Rev.* **2001**, *46*, 3-26, https://doi.org/10.1016/s0169-409x(00)00129-0.
38. Paolo, A.; Alessio, B.; Stefania, N.; Gabriella, F.; Riccardo, F.; Mauro, F. Allosteric Modulation of Drug Binding to Human Serum Albumin. *Mini-Rev. Med. Chem* **2006**, *6*, 483-489, https://doi.org/10.2174/138955706776361448.
39. Irvine, J.D.; Takahashi, L.; Lockhart, K.; Cheong, J.; Tolan, J.W.; Selick, H.E.; Grove, J.R. MDCK (Madin-Darby Canine Kidney) Cells: A Tool for Membrane Permeability Screening. *J. Pharm. Sci.* **1999**, *88*, 28-33, https://doi.org/10.1021/js9803205.
40. Sanguinetti, M.C.; Tristani-Firouzi, M. hERG potassium channels and cardiac arrhythmia. *Nature* **2006**, *440*, 463-469, https://doi.org/10.1038/nature04710.

Publisher's Note & Disclaimer